Materials Science & Engineering C 109 (2020) 110575

Contents lists available at ScienceDirect

Materials Science & Engineering C

journal homepage: www.elsevier.com/locate/msec

PEDOT-polyamine composite films for bioelectrochemical platforms - flexible and easy to derivatize

Luciano D. Sappia[a,1], Esteban Piccinini[a,1], Catalina von Binderling[a], Wolfgang Knoll[b,c,d], Waldemar Marmisollé[a,*], Omar Azzaroni[a,c,d,*]

[a] Instituto de Investigaciones Fisicoquímicas Teóricas y Aplicadas, Departamento de Química, Facultad de Ciencias Exactas, Universidad Nacional de La Plata, CONICET, CC 16 Suc. 4, La Plata B1904DPI, Argentina
[b] CEST - Competence Center for Electrochemical Surface Technologies, Konrad Lorenz Strasse 24, 3430 Tulln, Austria
[c] Austrian Institute of Technology - Donau-City-Strasse 1, 1220 Vienna, Austria
[d] CEST-UNLP Partner Lab for Bioelectronics, Diagonal 64 y 113, La Plata 1900, Argentina

ARTICLE INFO

Keywords:
Bioelectrochemistry
PEDOT
Glycoenzymes
Anti-fouling surfaces
Flexible sensors

ABSTRACT

We report a straightforward route for the preparation of flexible, electrochemically stable and easily functionalizable poly(3,4-ethylenedioxythiophene) (PEDOT) composite films deposited on PET foils as biosensing platforms. For this purpose, poly(allylamine) hydrochloride (PAH) was blended with PEDOT to provide amine-bearing sites for further biofunctionalization as well as to improve the mechanical properties of the films. The conducting PEDOT-PAH composite films were characterized by cyclic voltammetry, UV–vis and Raman spectroscopies. An exhaustive stability study was carried out from the mechanical, morphological and electrochemical viewpoint. Subsequent sugar functionalization of the available amine groups from PAH allowed for the specific recognition of lectins and the subsequent self-assembly of glycoenzymes (glucose oxidase and horseradish peroxidase) concomitant with the prevention of non-specific protein fouling. The platforms presented good bioelectrochemical performance (glucose oxidation and hydrogen peroxide reduction) in the presence of redox mediators. The developed composite films constitute a promising option for the construction of all-polymer biosensing platforms with great potential owing to their flexibility, high transmittance, electrochemical stability and the possibility of glycosylation, which provides a simple route for specific biofunctionalization as well as an effective antifouling strategy.

1. Introduction

Conjugated polymers (CPs) have emerged as a promising alternative to replace traditional metallic and carbon-based materials commonly used for electrode fabrication in bioelectronics [1]. Most strategies for the implementation of CPs in bioelectronics require their deposition on conductive substrates. However, metals and other rigid substrates can limit their use in some specific practical applications, like stretchable or implantable sensors [1,2]. This is the reason why there has been recently a considerable interest in the fabrication of “all-polymer” metal-free electrodes for bioelectronics and biosensing [3–7]. Additionally, the incorporation of enzymes to CPs-based devices provides selectivity, specificity and catalytic properties towards a determined target. In the case of affinity or catalytic biosensors, the immobilization of biomacromolecules is a key process that should be done avoiding the loss of biological activity while maximizing the accessibility to the active/recognition site [8]. Therefore, plenty of bioconjugation strategies of CPs has been developed, including physical entrapment (drop-casting, electropolymerization), layer-by-layer techniques, covalent attachment using cross-linking agents (glutaraldehyde, divinyl sulfone, EDS/NHS, tosil activated groups, etc.) and affinity-based immobilization methods (antibodies, aptamers, molecularly imprinted polymers, etc.) [8–11]. Within these methods, recognition-directed assembly allows effectively avoiding denaturalization while keeping the active sites fully exposed to the solution by mimicking recognition mechanisms found in nature [12–15].

Within CPs, poly(3,4-ethylenedioxithiophene) (PEDOT) constitutes a reference material to interface biotic/abiotic elements in

* Corresponding authors at: Instituto de Investigaciones Fisicoquímicas Teóricas y Aplicadas (INIFTA), Fac. de Cs. Exactas, Universidad Nacional de La Plata – CONICET, 64 y Diag. 113, 1900 La Plata, Argentina.
E-mail addresses: wmarmi@inifta.unlp.edu.ar (W. Marmisollé), azzaroni@inifta.unlp.edu.ar (O. Azzaroni).
[1] These authors contributed equally to this work.

https://doi.org/10.1016/j.msec.2019.110575
Received 15 October 2019; Received in revised form 13 December 2019; Accepted 19 December 2019
Available online 31 December 2019
0928-4931/

bioelectronics [1,16–18], used in a great variety of applications, such as medical biosensors [7,19], drug-delivery systems [20,21], stretchable electronic devices [22] and surfaces for controlling cell growth and attachment [23–25]. The implementation of PEDOT in such diverse fields is related to some advantages, such as low-cost of production, easy synthesis on metallic and plastic substrates [26], high conductivity (3300 to 5400 $S.cm^{-1}$ in some cases) [27–29], and adaptability to flexible and transparent substrates [28,30,31]. Furthermore, PEDOT properties can be easily modulated by selecting the suitable polymerization procedure and the counter anion or dopant nature [32,33], although it can be also modified by furhter post-biofunctionalization methods [34]. Concerning PEDOT post-biofunctionalization, most common procedures are based on the electropolymerization of EDOT and EDOT derivatives containing a recognition motif or an easily functionalizable functional group [35]. Alternatively, biomolecules can be also entrapped by electropolymerization using the monomer EDOT in solution. Nevertheless, the incorporation of macromolecules can decrease the conductivity of the PEDOT and/or the biomolecules can be irreversibly affected [36]. Otherwise, the integration of polyelectrolytes within the PEDOT matrix has been proved to be an effective strategy for conferring anchoring sites for further biofunctionalization without drastically disrupting its electronic properties. In this sense, Rozlosnik and coworkers have used hydroxyl-modified EDOT for the construction of impedimetric all-polymer sensors [37], and the incorporation of easily modifiable polymers like PSS-*co*-maleic acid or polyallylamine, produced stable hybrid composites retaining the added polymers to the PEDOT matrix by supramolecular interactions [4,38].

Following this last functionalization approach, in this work we present the construction and evaluation of flexible all-polymer electrodes based on the integration of PEDOT and polyallylamine hydrochloride (PAH) on PET substrates. Amine groups from PAH were used as anchoring sites for the glycosylation of the surfaces with mannose and N-Acetyl glucosamine via divinyl sulfone (DVS) chemistry. Then, Con A and wheat germ agglutinin (WGA) were selectively assembled on the glycosylated surfaces and the biorecognition interactions of these lectins with glucose oxidase (GOx) and horseradish peroxidase (HRP) were employed for the construction of bioelectroactive electrodes for glucose and H_2O_2 sensing. In that way, the synergistic combination of PEDOT and recognition-directed assembly of redox glyco-enzymes allowed for the building-up of all-polymer bioelectroactive flexible platforms.

2. Experimental details

2.1. Synthesis of PEDOT and PEDOT-PAH composite films

PEDOT films were deposited by spin-coating of the polymerization solution on PET foils (3 cm × 3 cm × 0.1 cm) as already reported [4]. The oxidant solution consisted of a mixture of iron (III) p-toluenesulfonate 40% wt in butanol (CB 40, Clevios™, Heraeus Holding GmbH, Hanau, Germany), butanol (ACS, Merck) and pyridine (ACS, Biopack) in a 1:0.3:0.023 ratio, respectively. Then, this solution was mixed with the EDOT monomer (97%, Sigma-Aldrich), filtered (pore size = 0.2 μm) and deposited by spin-coating (WS-650MZ-23NPP, Laurell) at 1000 rpm for 1 min with an acceleration of 500 $rpm.s^{-1}$. Finally, the substrates were heated at 50 °C for 15 min, washed in deionized water for 5 min and dried under N_2 flow [4,39,40].

For the preparation of PEDOT-PAH composites, 15 mg of polyallylamine hydrochloride (PAH) (58 kDa, Sigma Aldrich) was dissolved in 200 μL of deionized water and then mixed with 951.5 μL of the oxidant solution. The resulting oxidant solution was mixed vigorously and the EDOT monomer was added in a 1:0.013 ratio [4]. This solution was the filtered and deposited on the PET substrates by spin-coating under the same conditions described for pristine PEDOT films. At these conditions, films with a mass proportion of PAH to PEDOT of m(PAH)/m(PEDOT) = 1.34 are obtained, as previously determined by XPS [4].

2.2. Characterization of the PEDOT films

Sheet resistance measurements were carried out using a TEQ-03 potentiostat with a four-point probe (4PP) accessory (NanoTeq, Argentina). Five locations were measured for each sample and the average value with the standard deviation is reported. The effect of bending on the electrical properties of PEDOT and PEDOT-PAH films deposited on PET substrates was evaluated by measuring the resistance (Agilent 1241 U digital multimeter) after performing mechanical bending cycles.

An UV–Visible modular spectrometer Ocean Optics 4000 UV–Vis was used to evaluate the transmittance spectra of the samples. Raman spectra were acquired using i-Raman BW415-532S (BWTek) Raman spectrometer. The spectral region analyzed ranged from 100 to 4000 cm^{-1}. The excitation wavelength was 532 nm and the laser (power = 10 mW) was focused on the substrates by a 20× optical microscope (BAC151B, BWTek).

Cyclic voltammetry (CV) experiments were performed with a TEQ-03 potentiostat using a three-electrode cell equipped with an Ag/AgCl (3 M NaCl) reference electrode, a platinum wire counter electrode and the working electrode with an active area of 0.18 cm^2.

AFM images were acquired with a Multimode 8 AFM (Nanoscope V Controller, Bruker, Santa Barbara, CA). Tapping mode imaging was performed in a dry nitrogen environment by using silicon probes (RTESP, 40 N/m spring constant, 12 nm tip radius, Bruker). Image analysis and RMS roughness evaluation were performed using NanoScope Analysis software (Bruker).

Contact angle goniometry measurements (Ramé-Hart contact angle system, Model 290) were carried out to validate the sequential modification steps. For each system, 1 μL droplets of deionized water were dispensed five times in different positions of the sample. The average contact angle value and its standard deviation is reported.

2.3. Glycosylation of PEDOT-PAH surfaces and the self-assembly of lectins

PEDOT-PAH composites were glycosylated based on a protocol by Hatakeyama et al. [10] with some modifications [4]. Briefly, the protocol involved a first incubation step with 5% divinylsulfone (DVS, V3700, Sigma Aldrich) dissolved in carbonate buffer solution (0.5 M Na_2CO_3, pH 11) for 1 h and then the substrates were washed twice with carbonate buffer. After that, the substrates were incubated in 10% mannose (112,585, Sigma Aldrich) or 10% *N*-acetylglucosamine (GlcNAc) (A8625, Sigma Aldrich) carbonate buffer solutions for 18 h. Finally, the glycosylated surfaces were rinsed thoroughly with TBS buffer (10 mM Tris, 0.1 M NaCl, pH 7.5) and stored at 4 °C.

The recognition-driven assembly of Con A lectin on the mannosylated surfaces was carried out as previously reported [4,41]. Mannosylated PEDOT-PAH films were incubated for 30 min in a 1 μM Con A (MW = 104 kDa, C2010, Sigma Aldrich) solution containing 20 mM HEPES, 0.5 mM $CaCl_2$ and 0.5 mM $MnCl_2$ at pH 7.4. The buffer was supplemented with Ca^{2+} and Mn^{2+} to promote the Con A-carbohydrate recognition [42]. In a similar way, the lectin wheat germ agglutinin (WGA, 36 kDa, L9640, Sigma-Aldrich) was assembled onto GlcNAc/PEDOT-PAH films. The substrates were incubated for 30 min in a 1 μM WGA solution containing 20 mM HEPES at pH 7.4. WGA assembly and its stability were characterized by surface plasmon resonance spectroscopy (SPR) on gold substrates modified with GlcNAc by the DVS chemistry [4,10]. SPR experimental details are described in the supporting information (Section S3).

2.4. Glycoprotein-lectin recognition

Glucose oxidase (GOx, MW of 160 kDa, Aspergillus niger, 225 U/mg, Calzyme, USA) and horseradish peroxidase (HRP, MW of 44 kDa, P8375, Sigma-Aldrich) were assembled on the lectin-modified PEDOT-PAH platforms, by direct incubation of 1 μM glycoprotein solutions in

20 mM HEPES (and in the case of GOx, also containing 0.5 mM Ca^{2+} and 0.5 mM Mn^{2+}) at pH 7.4 for 30 min. In order to assess the non-specific adsorption, the glycosylated PEDOT-PAH films (without the subsequent lectin incubation step) were also incubated in the glycoproteins solutions.

2.5. Glucose and hydrogen peroxide bioelectrocatalysis

In the case of glucose, 100 μM ferrocenemethanol (FcOH) was employed as redox mediator in 0.1 M KCl and 20 mM HEPES buffer at pH 7.4 under N_2 atmosphere. Stock 1 M glucose solution was prepared at least one day before the measurements to reach the glucose mutarotation equilibrium [43]. In the case of hydrogen peroxide (H_2O_2, 30%, ACS, Merck), the bioelectrocatalysis was carried out using 1 mM hydroquinone (HQ, ACS, Merck) as a redox mediator in 0.1 M KCl and 20 mM HEPES buffer at pH 7.4. The HRP enzyme substrate H_2O_2 and HQ stock solutions were prepared daily.

3. Results and discussion

PEDOT-based films were deposited on flexible PET substrates by spin-coating of the precursor solutions and further oxidative polymerization. The construction steps for the PEDOT and PEDOT-PAH-modified platforms and the biofunctionalization procedures are depicted in Scheme 1.

3.1. Spectroscopic and electrical characterization of the PEDOT and PEDOT-PAH films

Fig. 1 shows comparative results of PEDOT ($PEDOT_{1L}$) and PEDOT-polyamine composite ($PEDOT\text{-}PAH_{1L}$) films deposited on PET foils. For comparison with our previous work, a multi-layer film was constructed by the deposition of two pristine PEDOT layers and a third layer of PEDOT-PAH composite ($PEDOT_{2L}/PEDOT\text{-}PAH_{1L}$). This three-layers coating was employed as reference as it was proved to present good electronic and mechanical properties when deposited on other plastic substrates. The thicknesses of the films were estimated from the SEM images as 2.8 ± 0.2 μm for the $PEDOT_{1L}$, 2.3 ± 0.4 μm for the $PEDOT\text{-}PAH_{1L}$ composite and 5 ± 0.4 μm for the multi-layer $PEDOT_{2L}/PEDOT\text{-}PAH_{1L}$ composite (Appendix, Fig. S1). The chemical nature of the deposited materials was confirmed by Raman spectroscopy (Fig. 1A). The Raman spectrum of a PEDOT layer deposited on glass, shows the typical peaks for PEDOT. The most intense peaks are found at 1365 cm^{-1} (assigned to C_β-C_β stretching), 1421 cm^{-1} (assigned to symmetric $C_\alpha = C_\beta(-O)$ stretching) and 1510/1563 cm^{-1} (assigned to asymmetric $C_\alpha = C_\beta$ stretching) [44–46]. In the case of clean PET foils substrates, there are two main bands at 1615 cm^{-1} and 1722 cm^{-1}, assigned to the symmetric stretching of 1,4 carbons of benzene rings and stretching modes of C═O bonds, respectively [47,48]. For the PEDOT and PEDOT-PAH films on PET, the spectra show the presence of all the peaks assigned for the pristine PEDOT. The presence of PAH within the composite material is revealed as a distortion of the band at about 1500 cm^{-1} caused by superposition of two main broad bands from amine groups (symmetric and anti-symmetric bending modes is protonated amines) and the broadening of the band at about 1360 cm^{-1} due to CH bending modes, as reported previously [4].

As can be seen in Fig. 1B, the addition of PAH to PEDOT decreases the sheet resistance by 47% (from 327 to 174 Ω/sq) if compared with the pristine PEDOT ($PEDOT_{1L}$). This change for $PEDOT\text{-}PAH_{1L}$, in comparison to $PEDOT_{1L}$, may be attributed to the rearrangement of the PEDOT polymer chains if PAH is added to the film what could yield to an improvement of the conductivity such as was reported for PEDOT:Tos with polyethylenglycol (PEG) [49] or PEDOT:PSS with ethylenglycol (EG) [50].

As commented above, the incorporation of PAH to PEDOT pursues the aim of conferring easily functionalizable groups for further chemical modifications of the platforms. Results in Fig. 1B indicate that no drastic alterations of the conductance are produced by the addition of the non-conducting PAH. However, in some applications, films with particularly low electric resistance could be required. In this particular case, a possible synthetic strategy could be the deposition of PEDOT/PAH on a PEDOT modified substrate. This strategy was explored by preparing the $PET/PEDOT_{2L}/PEDOT\text{-}PAH_{1L}$ platform. As expected, in the case of the $PET/PEDOT_{2L}/PEDOT\text{-}PAH_{1L}$ multilayer platform, the

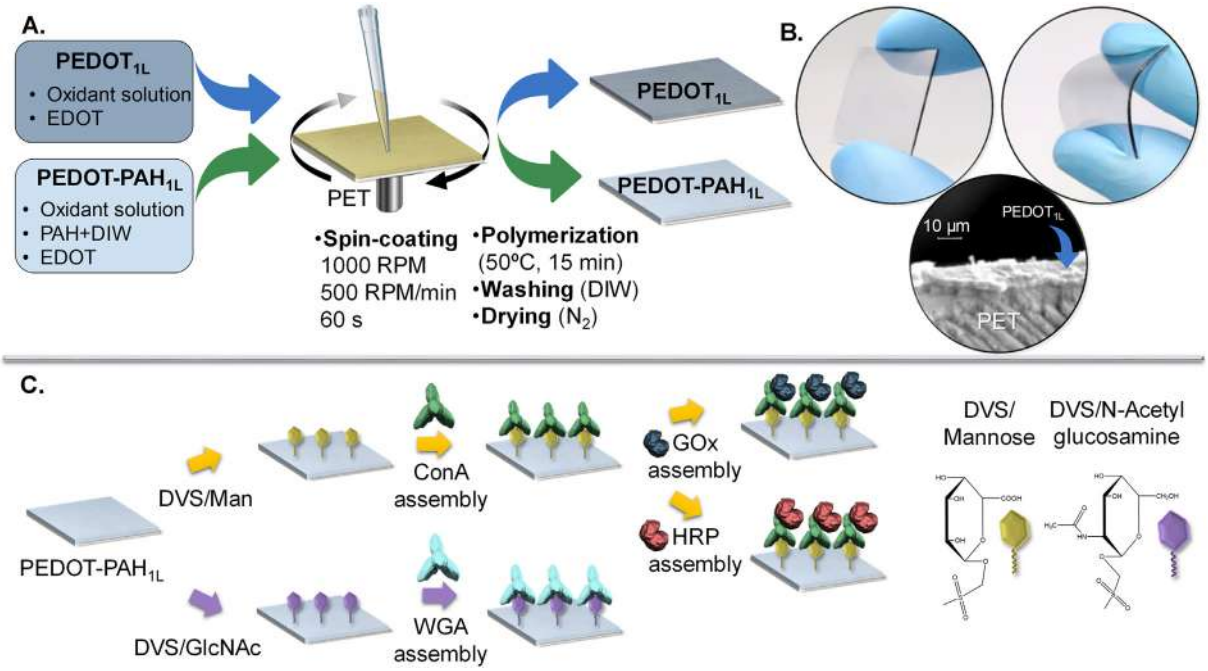

Scheme 1. (A) Preparation of $PEDOT_{1L}$ and $PEDOT\text{-}PAH_{1L}$ films by spin-coating on the PET foils. (B) Images of a PET foil substrate with a single layer of PEDOT-PAH as-deposited and in the bending state. (C) Sequential glyco-modification of a $PEDOT\text{-}PAH_{1L}$ composite by divinylsulfone chemistry and the sequential self-assembly of lectins and glyco-enzymes.

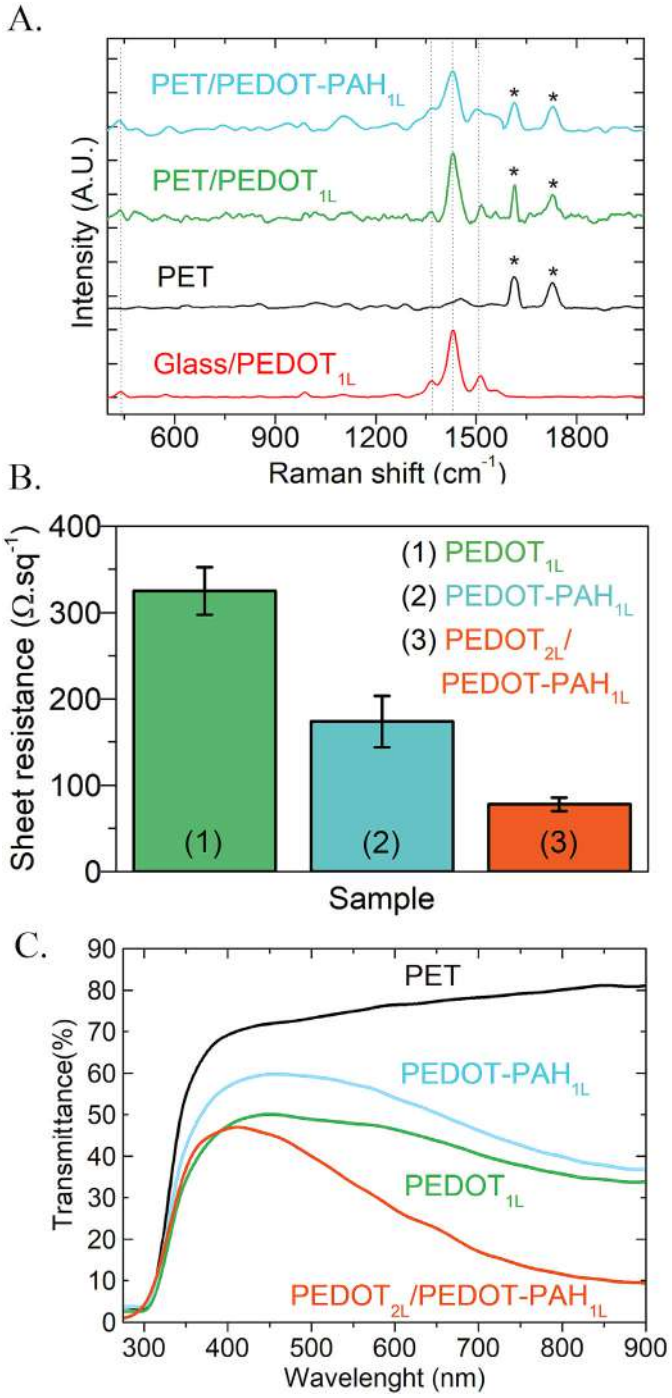

Fig. 1. (A) Raman spectra of pristine PEDOT and PEDOT-PAH composites prepared on glass and PET. (B) Sheet resistance measured by 4PP for PEDOT, PEDOT-PAH_{1L} and $PEDOT_{2L}$/PEDOT-PAH_{1L} composites deposited on PET substrates. (C) Transmittance spectra of the films deposited on PET substrates.

sheet resistance decreased to 78 Ω/sq. because of the addition of the two PEDOT conducting layers under the PEDOT-PAH one. Although better conductance is achieved by previous deposition of PEDOT layers, this method could also present some drawbacks, such as the increase in the preparation time, reagent consumptions and capacitive current and the lowering of the substrates transparency, as explored below.

Transparency features of the films deposited on PET foils are characterized by UV–Vis measurements in the wavelength range from 400 to 800 nm. Fig. 1C presents the transmittance (T%) spectra of the flexible substrates. If we compare the T% at 600 nm between different samples, the PET substrate presents a T% of 76, while after the deposition of the $PEDOT_{1L}$ and PEDOT-PAH_{1L} monolayers, T% decreases to 47 and 55, respectively. In the case of the multilayer sample (PET/$PEDOT_{2L}$/PEDOT-PAH_{1L}) the transmittance decreases to 28. These results indicate that PEDOT and PEDOT-PAH films on PET present high transmittance in the visible range, which made them adequate platforms for optical applications. Of course, transparency decreases when increasing the number of polymer layers deposited. The present results are comparable to other ones reported for similar systems. For instance, Sanglee et al., reported a T% at 600 nm for glass (81), polyester substrate + PEDOT:PSS monolayer (80), polyester substrate + PEDOT:PSS monolayer + poly (3-hexylthiophene) (60) [51]. Li and Ma developed a liquid phase deposition method to generate PEDOT films on PET directly by the immersion of a PET foil in an 80 mM $FeTos_3$ in butanol for 10 min, then the films are dried for 3 min at 40 °C and then immersed in an 80 mM EDOT in cyclohexane solution for 15–20 h [31]. They obtained a monolayer film on PET with a T% of 81–86 at 550 nm, a sheet resistance of 200–260 Ω/area and a thickness of 100 nm. Hu et al. used a highly transparent PET mesh as substrates. Then, PEDOT PSS was deposited by 8 printing cycles on the PET mesh obtaining a sheet resistance of 245 Ω/sq., the substrate presented a T% (at 550 nm) of 46 (before deposition) and 20 after 8 printing cycles [52].

The mechanical stability was evaluated by measuring the electrical resistance as a function of the number of mechanical bending cycles. The bending was performed until 108°, which was verified to be the maximum angle without exceeding the elastic limit of the PET foil is reached. In Fig. 2, the percentage change in the resistance (%ΔR/Ri) is plotted as a function of the bending cycles for $PEDOT_{1L}$ and PEDOT-PAH_{1L}. After 100 bending cycles, the pristine PEDOT showed a resistance increase of 14.2 ± 8.1% (n = 3), whereas for the PEDOT-PAH films the resistance increased only 1.2 ± 0.4% (n = 3). These results indicate that PEDOT-PAH composites showed a better mechanical stability than pristine PEDOT probably due to an improved film adhesion and/or higher elasticity of the composite material.

3.2. Electrochemical behavior of PEDOT and PEDOT-PAH films

Fig. 3 presents the voltammetric behavior of $PEDOT_{1L}$, PEDOT-PAH_{1L} and $PEDOT_{2L}$/PEDOT-PAH_{1L} using 1 mM FcOH as a redox probe at different scan rates. In all cases, voltammograms present the same aspect, indicating the behavior of the redox probe is almost the same. Moreover, although current values increases with the thickness of the

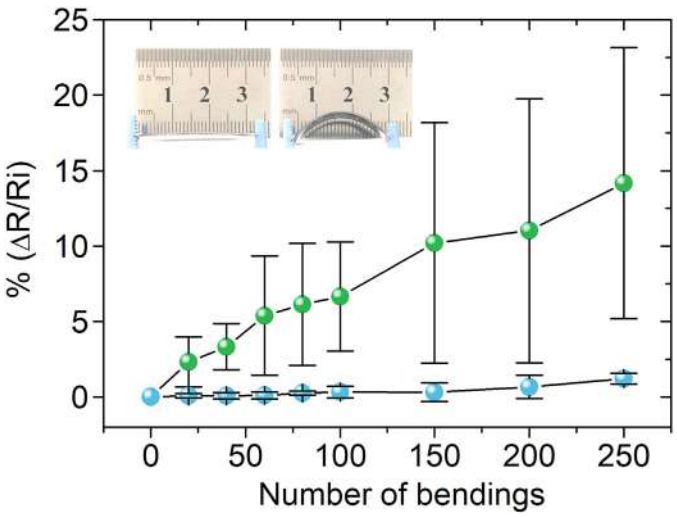

Fig. 2. Changes in resistance of $PEDOT_{1L}$ (green) and PEDOT-PAH_{1L} (blue) onto PET substrates for increasing number of bending cycles. (For interpretation of the references to colour in this figure legend, the reader is referred to the web version of this article.)

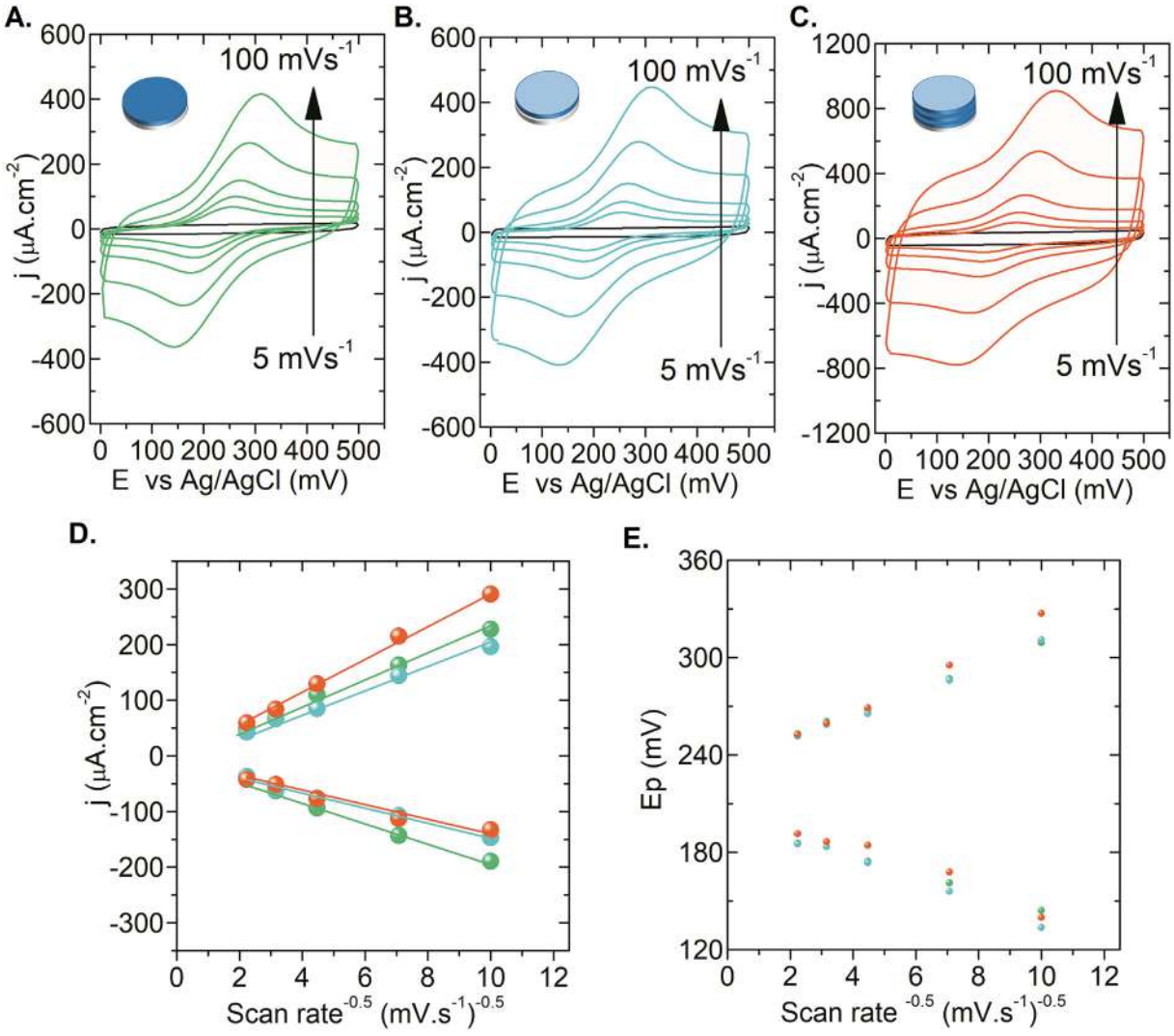

Fig. 3. Cyclic voltammograms of $PEDOT_{1L}$ (A), $PEDOT\text{-}PAH_{1L}$ (B) and $PEDOT_{2L}$/$PEDOT\text{-}PAH_{1L}$ (C) in 1 mM FcOH at different scan rates (5, 10, 20, 50 and 100 mV s^{-1}). (D) Anodic and cathodic peak current density as a function of the square-root of the scan rate. (E) Peak potentials for increasing scan rates. Colour code from panels A-C is maintain in panels D and E.

polymer layer (higher capacitive contributions), when comparing background-subtracted peak current values, they are quite similar for all the platforms (Fig. 3D). Furthermore, for all the cases, the background-subtracted peak current density (j_p) increases linearly with the square root of the scan rate ($\upsilon^{1/2}$) which indicates that the electrochemical reaction of FcOH is controlled by a semi-infinite linear diffusion (Fig. 3D) [53]. No adsorption of the redox couple was observed independently of the presence of PAH in the films (Fig. S2). As it is shown in Fig. 3E, the separation between the anodic and cathodic peak potential increases with υ (characteristic of quasi-reversible electrochemical systems) [53] in a similar manner for the three systems, evidencing that the electron transfer rates between the redox probe and the conducting film does not fall away by the addition of PAH neither by the simplification of the platform from three to one conducting layers.

As mentioned above, the capacitive contribution of the current density in the multilayer system was higher than the monolayer systems, whereas the faradaic contribution remains almost constant (Figs. S2 and S3). This is an expected behavior as the capacitive contribution of conducting polymer films is proportional to the polymer mass [54]. As it is shown in the following section, the capacitive contribution could present severe implications for the construction of bio-electrosensing devices.

The electrochemical stability of the PEDOT and PEDOT-PAH films was also evaluated by cyclic voltammetry in the presence of 1 mM FcOH. Fig. 4 presents the voltammograms of PEDOT and PEDOT-PAH for increasing number of voltammetric cycles. For both systems, the redox current densities of the films remain almost constant throughout 300 cycles, indicating that the conducting platform is electrochemically stable. Moreover, the film topography was studied by AFM before and after the 300 voltammetric cycles. The pristine PEDOT films did not show appreciable changes of the RMS roughness before (3.5 ± 0.2 nm) and after (3.3 ± 0.2 nm) the electrochemical procedure. Contrarily, $PEDOT\text{-}PAH_{1L}$ films showed a decrease of the RMS roughness from 4.3 ± 0.7 nm to 1.96 ± 0.05 nm after the 300 cyclic voltammograms. This last fact could be related to the rearrangement of more flexible polymer fibers of the composite compared to PEDOT [55].

On the other hand, the voltammetric performance after mechanical bending of the platforms was also evaluated. After the bending cycles, the central area of each film was cycled in 1 mM FcOH. Results presented in the Appendix indicate that the voltammograms showed almost no difference in terms of current density and CV shape compared to those obtained before the bending experiments (Fig. S4).

It is worth pointing out that, in the presence of a redox probe, $PEDOT\text{-}PAH_{1L}$ monolayer showed similar electron transfer rate than $PEDOT_{1L}$ but an improvement of the electrical conducting stability

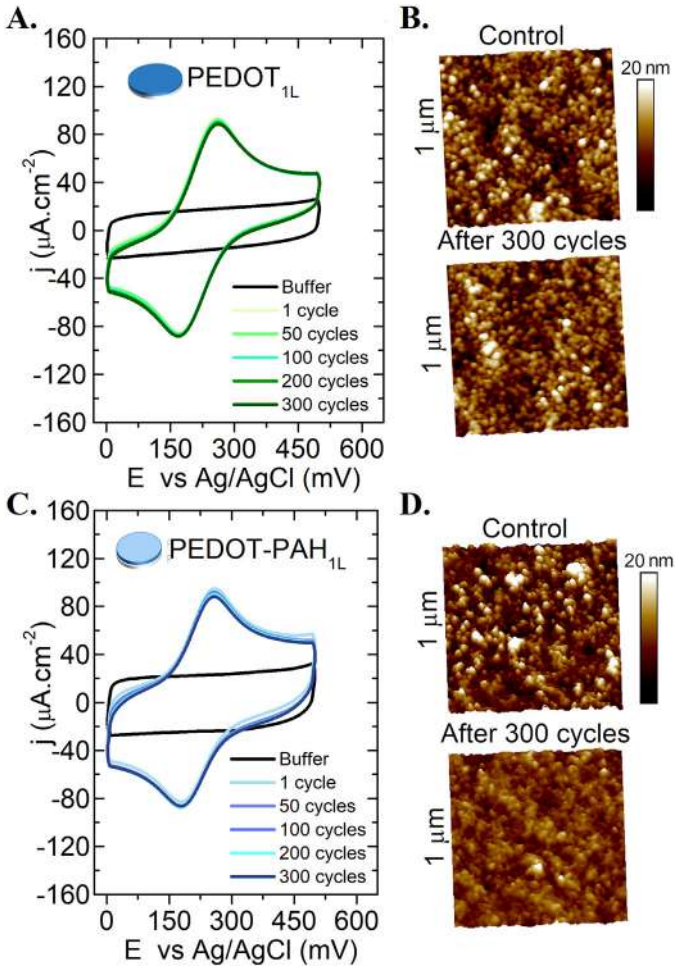

Fig. 4. Electrochemical stability of PEDOT (A) and PEDOT-PAH (C) films. Each system was studied throughout 300 voltammetric cycles at 10 mV s^{-1} in 1 mM FcOH in buffer HEPES. AFM images (1 × 1 μm) taken in tapping mode before and after the electrochemical cycling for PEDOT (B) and PEDOT-PAH films (D).

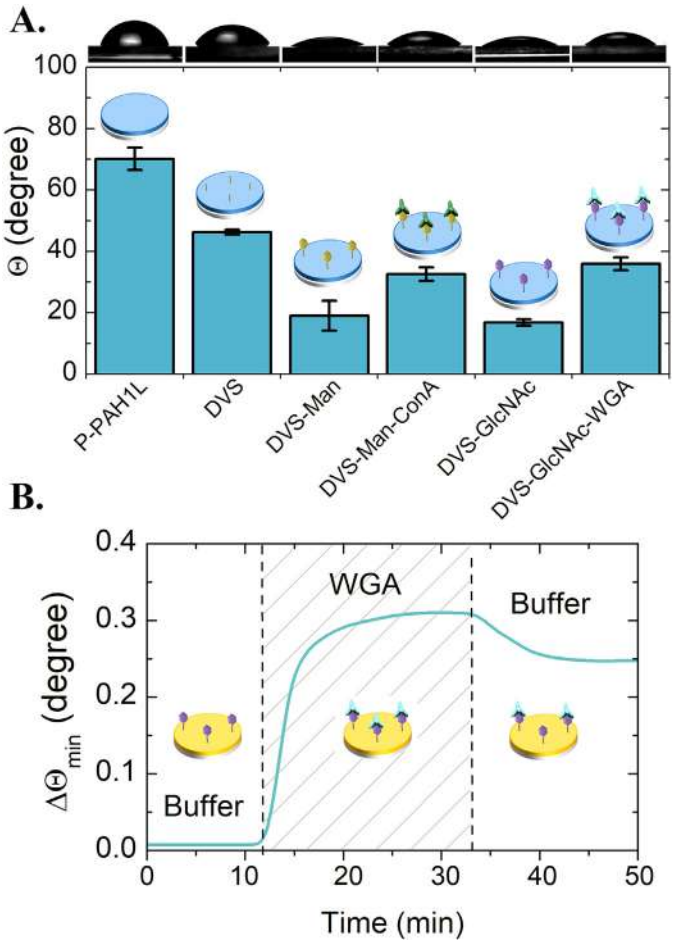

Fig. 5. (A) Contact angle goniometry was used to monitor DVS, Man/GlcNAc sugars and Con A/WGA lectins modifications of the PEDOT-PAH_{1L} films prepared on PET. P-PAH_{1L} = PEDOT-PAH monolayer on a PET foil, DVS = divinylsulfone, Man = Mannose, Con A = Concanavalin A, GlcNAc = *N*-acetyl-d-glucosamine, WGA = Wheat germ agglutinin (B) Time-resolved SPR sensogram for WGA self-assembly onto a GlcNAc-modified SPR sensor. The experiment was performed using a 785 nm laser and a flow rate of 10 μL.min^{-1}. Buffer = 20 mM HEPES, 0.1 M KCl and pH 7.4.

when the substrates were submitted to mechanical bending cycles. Moreover, PEDOT-PAH_{1L} platforms are not only easier to prepare than $PEDOT_{2L}$/PEDOT-PAH_{1L} platforms but they also showed lower capacitance, what is a necessary feature for sensing applications [40]. Owing to the excellent mechanical and electrochemical stability of PEDOT-PAH films on PET, this platform seems to be promissory for the development of reliable all-polymer and flexible bioelectronic devices. Thus, in the following sections, we explore the biofunctionalization of the single PEDOT-PAH configuration.

3.3. Glycosylation of PEDOT-PAH surfaces for lectin self-assembly

Having in mind the design of flexible and low-cost electrochemical biosensing devices, we explore the self-assembly of lectins and glycoenzymes mediated by carbohydrate-lectin recognition onto the PEDOT-PAH platforms. Firstly, we proceeded to the covalent anchoring of sugar motifs to the PEDOT-PAH platform. To achieve this task, divinylsulfone (DVS) chemistry was exploited for the glycosylation of the primary amines from the PAH integrated into the film, as demonstrated before [4,10]. This straightforward synthetic route involves two sequential nucleophilic 1,4-additions, wherein DVS serves as a cross-linker between the nucleophilic group of the surface (-NH_2) and the nucleophilic group of the carbohydrate (-OH) [56–58].

Owing to the high hydrophilic character of carbohydrates, glycosylation via DVS can be proved measuring the wettability changes [57]. Fig. 5A shows the contact angle measurements before and after the glycosylation of the PEDOT-PAH films, as well as along the lectins self-assembly procedure (Table S1). Before DVS modification, the PEDOT-PAH_{1L} monolayer showed a contact angle of 70 ± 3°. After the incubation in DVS, the modification of the surface is evidenced by the decrease of the contact angle to 46 ± 1°. In the subsequent step, DVS reacted with mannose or GlcNAc, resulting in a remarkable increase in hydrophilicity (contact angles were 18.9 ± 4.8° and 16.8 ± 1.1°, respectively) attributed to the sugar hydroxyl groups exposed to the surface [57,59].

The self-assembly of Concanavalin A (Con A) and Wheat germ agglutinin (WGA) lectins on the glycosylated (mannose or GlcNAc, respectively) PEDOT-PAH films was then studied. Lectins are proteins which bind determined monosaccharides with high specificity [10,43,60,61]. As it is well-known, the WGA lectin presents high affinity for GlcNAc and minor affinity for mannose [58,60,61]. On the other hand, Con A presents the highest affinity for mannose moieties [10,60]. After Con A and WGA self-assembly on mannose and GlcNAc-modified films respectively, the hydrophobicity increased due to the attachment of the proteins to the sugar motifs (Fig. 5A). The functionalization of PEDOT-PAH films was also monitored by EIS in 0.1 M KCl solution (Fig. S5), observing an increment of the high frequency and polarization resistances after the successive steps as a consequence of

the surface blocking with insulating materials.

Surface plasmon resonance (SPR) spectroscopy was employed for testing the lectin self-assembly in terms of surface coverage and stability. SPR spectroscopy is a useful and sensitive method to study biorecognition events in real time [62,63]. As PEDOT films present strong absorption in the visible range, the glycosylation protocol was performed on Au substrates modified with an amine-functionalized thiols (cysteamine), using the same conditions as those for PEDOT-PAH films. Employing this strategy, we have recently studied the Con A recognition on mannosylated-gold SPR sensors modified via the DVS chemistry [4]. We have now studied the WGA assembly following the same strategy. For this purpose, gold substrates were modified with GlcNAc and the angle of minimum reflectivity (θ_{min}) was monitored during the WGA self-assembly (Fig. 5B). WGA surface coverage (Γ) was estimated from the change of θ_{min} before and after the injection of the lectin solution. The $\Delta\theta_{min}$ for the WGA assembly was 0.242°; that is a surface coverage of 253 ng cm^{-2}, i.e., 7.02 pmol cm^{-2} (see SPR experimental details and calculations in the Appendix). This value is slightly smaller than those reported by Lienemann et al. [60]. After the WGA assembly, the lectin-sugar interaction was evaluated exposing the surface to a high concentration of a WGA binding-sites competing agent (100 mM GlcNAc), yielding only 13% of lectin desorption (Fig. S6). This high affinity between the WGA and the GlcNAc-modified surface is in agreement with previous works on other substrates [61]. For example, Lienemann and co-workers reported that WGA has a higher affinity towards the immobilized GlcNAc-self-assambled monolayers (SAMs) than towards the soluble free monosaccharide. These authors suggested the possibility of multivalent recognition between WGA and the glycosylated surface [60], because WGA presents up to three carbohydrate-binding sites.

The strategy of biorecognition-driven functionalization of the PEDOT-based platforms was validated by the assembly of two model glycoenzymes (GOx and HRP) via biorecognition interactions with Con A and further electrochemical detection of glucose and hydrogen peroxide.

3.4. GOx biorecognition and glucose bioelectrocatalysis

Glucose oxidase is a dimeric protein (160 kDa) with a 16%wt carbohydrate residue content (mainly mannose (80%) but also galactose and glucosamine) [64]. The bioelectrocatalytic response towards glucose oxidation was studied by cyclic voltammetry in the presence of FcOH as redox mediator [65]. The bioelectrocatalytic glucose oxidation is compared for the Con A/GOx assemblies onto $PEDOT_{2L}$/$PEDOT\text{-}PAH_{1L}$ and $PEDOT\text{-}PAH_{1L}$ platforms in Fig. 6A and B, respectively. The mannosylated-PEDOT-PAH films showed an increased current response towards the addition of glucose, evidencing the correct GOx self-assembly onto the Con A layer. Since the experiments were carried out in the absence of O_2, the rise of the faradaic current in the anodic wave was only triggered by the FcOH-mediated glucose oxidation. Before glucose addition, the redox reaction of the mediator FcOH corresponds to a quasi-reversible response. By comparing the results in Fig. 6A and B, it could be concluded that both systems present similar values of the catalytic currents. However, higher capacitive contribution is clearly noted in the case of the multilayer substrate, as commented above. Thus, the relative increase in the bioelectrocatalytic current is higher for the case of $PEDOT\text{-}PAH_{1L}$ in comparison with the multilayer platform. Working with thin base electrode films thus allows gaining sensitivity towards small faradaic changes (biosensing output), avoiding voltammetric distortions caused by the presence of a relatively high capacitive contribution frequently found in the case of thicker conducting polymer films [54].

On the other hand, the non-specific adsorption of GOx was evaluated on a mannosylated-$PEDOT\text{-}PAH_{1L}$ substrate without the Con A incubation step. As shown voltammograms in Fig. 6C, the catalytic contribution up to 100 mM glucose is almost negligible. This result

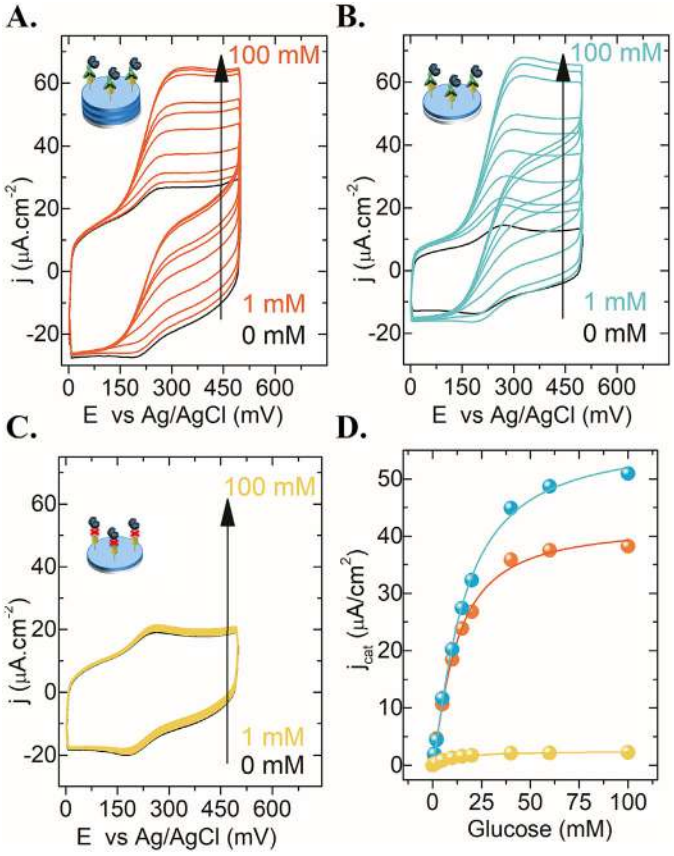

Fig. 6. Cyclic voltammograms of the bioelectrocatalysis of glucose oxidation at the Con A/GOx assembly on mannosylated-$PEDOT_{2L}$/$PEDOT\text{-}PAH_{1L}$ (A) and -$PEDOT\text{-}PAH_{1L}$ (B). The non-specific adsorption of GOx was evaluated on a mannosylated-$PEDOT\text{-}PAH_{1L}$ monolayer without the Con A incubation step (C). Background-subtracted bioelectrocatalytic current as a function of the substrate concentration for the 3 systems (D). Conditions: 100 μM FcOH in 0.1 M KCl, 20 mM HEPES buffer, pH 7.4 deoxygenated with N_2, ν = 5 $mV.s^{-1}$, glucose concentrations: 1, 2, 5, 10, 15, 20, 40, 60 and 100 mM.

evidences that the PEDOT-PAH mannosylation gives a way not only for the specific lectin recognition but also for avoiding the non-specific adsorption of proteins. This observation is in agreement with those reported for other glycosylated surfaces such as maltose-terminated or galactose-terminated thiol monolayers [66–68].

The bioelectrocatalytic current contribution (j_{cat}) was obtained by subtracting the redox mediator current obtained in the absence of glucose (black lines in Fig. 6). In the presence of glucose, this bioelectrocatalytic anodic current reaches a plateau at ca. 340 mV (Figs. S7 and S8). In Fig. 6D the dependence of the j_{cat} current at 340 mV is plotted as a function of the glucose concentration, yielding the typical response for enzyme-catalyzed bioelectrochemical reactions. At low substrate concentrations there is a linear increment on the catalytic current on the substrate concentration, whereas at high concentrations a plateau is obtained owing to the enzyme saturation. Particularly, the Con A/GOx assemblies on mannosylated interfaces exhibited a linear range up to 10 mM (Fig. S9) with a sensitivity of 2.05 (R^2 = 0.997) and 1.86 (R^2 = 0.987) μA cm^{-2} mM^{-1} for $PEDOT\text{-}PAH_{1L}$ and $PEDOT_{2L}$/$PEDOT\text{-}PAH_{1L}$ platforms respectively. These sensitivity values are comparable to those reported for different GOx/PEDOT-based architectures on conducting electrodes, such as gold [69], graphite [70] and ITO [71].

3.5. HRP biorecognition and hydrogen peroxide bioelectrocatalysis

HRP structure (44 kDa) consists of a single chain polypeptide with

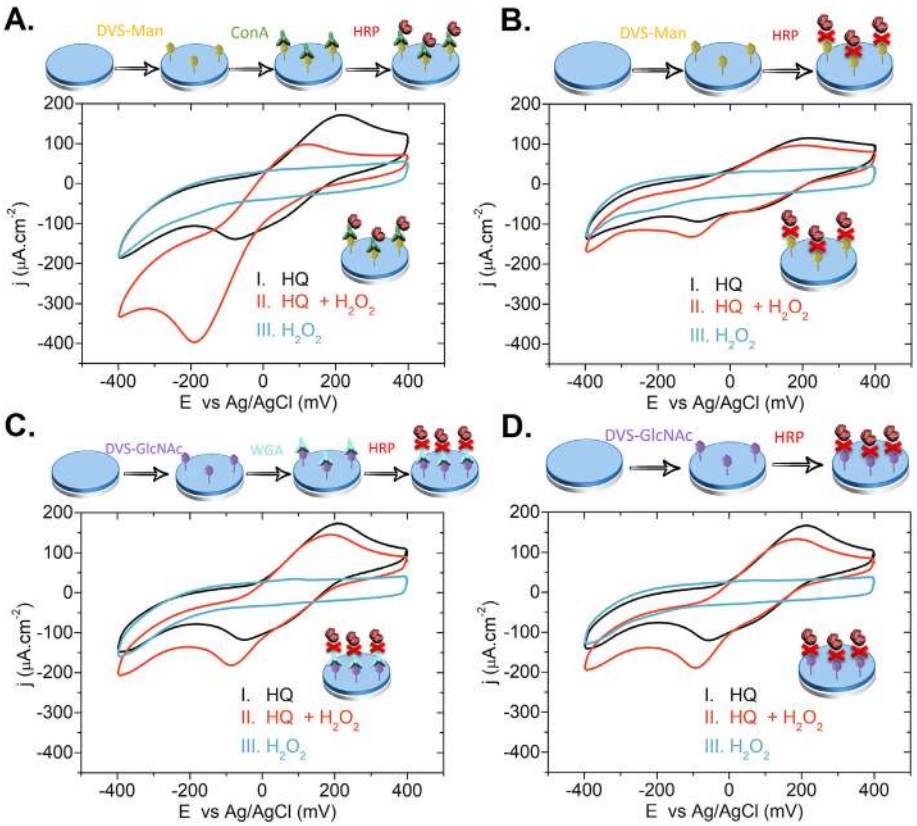

Fig. 7. H_2O_2 bioelectrocatalysis onto HRP-incubated platforms with different configurations: (A) PEDOT-PAH_{1L}/Man/ConA (B) PEDOT-PAH_{1L}/Man, (C) PEDOT-PAH_{1L}/ GlcNAc/WGA, (D) PEDOT-PAH_{1L}/ GlcNAc. The absence of bioelectrocatalytic signal for H_2O_2 reduction onto the glycosylated surfaces is indicative of the anti-fouling properties of these films; whereas the high signal obtained with the lectin Con A relative to WGA indicates the high specificity for the HRP sugar content. Conditions: 20 mM HEPES, 0.1 M KCl, pH 7.4, υ = 10 mV s^{-1}, [H_2O_2] = 2.5 mM, [HQ] = 1 mM.

four disulfide bridges, with 18% of carbohydrates content [72]. The nature of the sugar residues depends on the specific isozyme, and the monosaccharides galactose, arabinose, xylose, fructose, mannose, mannosamine, and galactosamine have been reported [73]. Owing to the superior performance of PEDOT-PAH_{1L} in comparison to the multilayer films in terms of the lower capacitive contribution, Con A and WGA were assembled onto the glycosylated-PEDOT-PAH_{1L} composites to explore the further assembly of HRP based on their specific sugar content. HRP assembly onto the glyco-surfaces was performed in absence of the cofactor Mn^{2+}, because it has been identified as an inhibitor of the enzyme [74].

Several redox mediators for HRP enzyme were reported in the construction of hydrogen peroxide biosensors, including ferro/ferricyanide salts, ferrocene and its derivatives (FcOH and FcCOOH), quinone and its derivatives [75–78]. Laschi and coworkers evaluated the suitability of hydroquinone (HQ), ferrocenemethanol and ferrocene monocarboxylic acid in PBS as redox mediators for HRP in solution. The authors reported that the current intensity increased 3 times for HQ when compared with ferrocene-based mediators [79]. Consequently, HQ was chosen as redox mediator, and its electrochemistry was studied on a PEDOT-PAH_{1L} electrode by CV. The optimal concentration of HQ (1 mM) for the bioelectrochemical reduction of H_2O_2 studies was also obtained from previous reports [80]. The redox mechanism for this mediator is also well-known (Section A.4).

Hydroquinone undergoes a quasi-reversible redox behavior on PEDOT-PAH_{1L} films, as it is revealed by the separation between the peak potentials (ΔEp = 106 mV) and the ratio between redox peak currents, I_{pa}/I_{pc} = 0.99 (Fig. S10). These results are similar to those obtained for HQ in aqueous solution by using gold or carbon working electrodes [78,79,81]. The addition of 1 mM H_2O_2 to the solution did not affect the HQ electrochemical redox reaction on the PEDOT-PAH_{1L} electrode (green and black lines of Fig. S11). However, in the presence of 1 μM HRP and 1 mM HQ, the addition of 1 mM H_2O_2 effectively caused the appearance of catalytic cathodic current (Fig. S11) [79]. This cathodic current was even more evident for 2.5 mM H_2O_2, meaning that it is caused by the HQ-mediated hydrogen peroxide reduction catalyzed by HRP [78], proving the effectiveness of the platform for bioelectrochemical transduction previously to the study on the system prepared by HRP assembled to the different functionalized PEDOT-PAH electrodes.

The bioelectroactivity of HRP assemblies on these PEDOT-PAH platforms and the specificity of its biorecognition interactions were then studied by measuring the H_2O_2 reduction activity on different configurations. Firstly, the peroxidase activity was tested by assembling HRP on Con A-functionalized platforms (PEDOT-PAH_{1L}/Man/Con A). As reported in Fig. 7A, before the addition of H_2O_2, the electrochemical response for 1 mM HQ presents a shift of the HQ reduction potential, which is attributed to the glycosylation and assembly on the PEDOT-PAH film. As shown in Fig. S10, the electrochemistry of HQ redox reaction is described by a quasi-reversible diffusion-governed charge transfer on the PEDOT surface [82]. The assembly of sugars and proteins decrease the electron transfer rate on the PEDOT surface, as it is shown in Fig. 7A. When 2.5 mM H_2O_2 was added, the reduction current increased with a maximum peak around −200 mV vs. Ag/AgCl, due to the HQ-mediated catalytic reduction of H_2O_2 by the assembled HRP. There was no current increase in the absence of HQ, which indicates that the electrochemical reaction is effectively mediated by HQ.

The specificity of the lectin-glycoenzyme interaction was also studied by employing the lectin WGA, which has a lower affinity for HRP residues [73]. WGA-functionalized platforms presented a negligible catalytic current for H_2O_2 reduction, indicating minor HRP adsorption (Fig. 7C). On the other hand, there were no significant changes in the cathodic current after the direct HRP incubation on glycosylated films with mannose (Fig. 7B) and GlcNAc (Fig. 7D), suggesting the absence of non-specific adsorption of the glycoenzyme. These results reinforce the idea that, as observed for GOx, the glycosylation of the conducting polymer film avoids any non-specific adsorption of proteins without the need of the common BSA blocking step. This property is of major

interest for electrochemical biosensing applications [83].

4. Conclusion

Herein we presented a simple strategy to modify PET foils with PEDOT-PAH composite films, for the construction of functionalizable and flexible all-polymer biosensing platforms. The PEDOT-PAH single layer electrode improves the multilayer platform ($PEDOT_{2L}$/$PEDOT\text{-}PAH_{1L}$) in terms of flexibility, transparency, cost and time of preparation. Moreover, as compared with the multilayer platforms, the simplified system presented similar electrochemical stability but lower capacitive contribution, yielding higher proportion of the useful bioelectrochemical current. We have also extended the use of these all-plastic sensing platforms, exploring the WGA and the glyco-enzyme HRP assemblies through supramolecular biorecognition-interactions yielding functional bioelectrochemical electrodes with antifouling properties.

In summary, we have presented an alternative strategy to construct all-polymer electrodes with good mechanical and electrochemical properties, able of being functionalized with lectins and glyco-enzymes by taking advantage of the presence of free amine groups. Such properties make these plastic substrates good candidates for the construction of bioelectrochemical devices in a variety of applications. The chemical richness of primary amine groups opens the door to future studies involving the rational modification of these electroactive platforms by integrating other building blocks for gaining additional functionalities.

Declaration of competing interest

The authors declare that they have no known competing financial interests or personal relationships that could have appeared to influence the work reported in this paper. The authors declare that they have no conflict of interest.

Acknowledgements

This work was supported by CONICET (PIP0370), ANPCyT (PICT-2016-1680, PICT-2017-1523), CEST-Competence Center for Electrochemical Surface Technologies (CEST − UNLP Partner Lab for Bioelectronics), Universidad Nacional de La Plata (PPID-X016).

Appendix A. Supplementary data

Supplementary data is available online containing additional results on the electrochemical characterization of PEDOT-based substrates, further surface functionalization, hydroquinone electrochemistry, and glucose and H_2O_2 bioelectrocatalysis optimizations. Supplementary data to this article can be found online https://doi.org/10.1016/j.msec.2019.110575.

References

[1] E. Zeglio, A.L. Rutz, T.E. Winkler, G.G. Malliaras, A. Herland, Conjugated polymers for assessing and controlling biological functions, Adv. Mater. 1806712 (2019) 1806712.
[2] J. Ha, S. Chung, M. Pei, K. Cho, H. Yang, Y. Hong, One-step interface engineering for all-inkjet-printed, all-organic components in transparent, flexible transistors and inverters: polymer binding, ACS Appl. Mater. Interfaces 9 (2017) 8819–8829.
[3] N.Y. Shim, D.A. Bernards, D.J. Macaya, J.A. DeFranco, M. Nikolou, R.M. Owens, et al., All-plastic electrochemical transistor for glucose sensing using a Ferrocene mediator, Sensors 9 (2009) 9896–9902.
[4] L.D. Sappia, E. Piccinini, W. Marmisollé, N. Santilli, E. Maza, S. Moya, et al., Integration of biorecognition elements on PEDOT platforms through Supramolecular interactions, Adv. Mater. Interfaces 4 (2017) 1700502.
[5] S.K. Kanakamedala, H.T. Alshakhouri, M. Agarwal, M.A. Decoster, A simple polymer based electrochemical transistor for micromolar glucose sensing, Sensors Actuators B Chem. 157 (2011) 92–97.
[6] L. Meng, A.P.F. Turner, W. Cheung Mak, Soft and flexible material-based affinity sensors, Biotechnol. Adv. (2019), https://doi.org/10.1016/j.biotechadv.2019.05.004 (pii: S0734-9750(19)30079-5).
[7] Y. Hui, C. Bian, S. Xia, J. Tong, J. Wang, Synthesis and electrochemical sensing application of poly(3,4-ethylenedioxythiophene)-based materials: a review, Anal. Chim. Acta 1022 (2018) 1–19.
[8] N. Stephanopoulos, M.B. Francis, Choosing an effective protein bioconjugation strategy, Nat. Chem. Biol. 7 (2011) 876–884.
[9] F.J. Lopez-Jaramillo, M. Ortega-Munõz, A. Megia-Fernandez, F. Hernandez-Mateo, F. Santoyo-Gonzalez, Vinyl sulfone functionalization: a feasible approach for the study of the lectin-carbohydrate interactions, Bioconjug. Chem. 23 (2012) 846–855.
[10] T. Hatakeyama, K. Murakami, Y. Miyamoto, N. Yamasaki, An assay for Lectin activity using microtiter plate with chemically immobilized carbohydrates, Anal. Biochem. 237 (1996) 188–192.
[11] F.H.M. Ali, M.I. Pividori, A.H.A. Hassan, L. Sappia, S.L. Moura, W.A. Moselhy, et al., Biomimetic magnetic sensor for electrochemical determination of scombrotoxin in fish, Talanta 194 (2018) 997–1004.
[12] M. Sarikaya, C. Tamerler, A.K.-Y. Jen, K. Schulten, F. Baneyx, Molecular biomimetics: nanotechnology through biology, Nat. Mater. 2 (2003) 577–585.
[13] D. Pallarola, N. Queralto, F. Battaglini, O. Azzaroni, Supramolecular assembly of glucose oxidase on concanavalin A—modified gold electrodes, Phys. Chem. Chem. Phys. 12 (2010) 8071–8083.
[14] E. Piccinini, D. Pallarola, F. Battaglini, O. Azzaroni, Recognition-driven assembly of self-limiting supramolecular protein nanoparticles displaying enzymatic activity, Chem. Commun. 51 (2015) 14754–14757.
[15] R.E. Giménez, E. Piccinini, O. Azzaroni, M. Rafti, Lectin-recognizable MOF glyconanoparticles: supramolecular glycosylation of ZIF-8 nanocrystals by sugar-based surfactants, ACS Omega 4 (2019) 842–848.
[16] S. Park, Y.J. Kang, S. Majd, A review of patterned organic bioelectronic materials and their biomedical applications, Adv. Mater. 27 (2015) 7583–7619.
[17] S. Kirchmeyer, K. Reuter, Scientific importance, properties and growing applications of poly(3,4-ethylenedioxythiophene), J. Mater. Chem. 15 (2005) 2077–2088.
[18] L. Groenendaal, F. Jonas, D. Freitag, H. Pielartzik, J.R. Reynolds, Poly(3,4-ethylenedioxythiophene) and its derivatives: past, present, and future, Adv. Mater. 12 (2000) 481–494.
[19] N. Rozlosnik, New directions in medical biosensors employing poly(3,4-ethylenedioxy thiophene) derivative-based electrodes, Anal. Bioanal. Chem. 395 (2009) 637–645.
[20] G. Kaur, R. Adhikari, P. Cass, M. Bown, P. Gunatillake, Electrically conductive polymers and composites for biomedical applications, RSC Adv. 5 (2015) 37553–37567.
[21] R. Wadhwa, C.F. Lagenaur, X.T. Cui, Electrochemically controlled release of dexamethasone from conducting polymer polypyrrole coated electrode, J. Control. Release 110 (2006) 531–541.
[22] L.V. Kayser, D.J. Lipomi, Stretchable conductive polymers and composites based on PEDOT and PEDOT:PSS, Adv. Mater. 31 (2019) 1806133.
[23] E.M. Stewart, M. Fabretto, M. Mueller, P.J. Molino, H.J. Griesser, R.D. Short, et al., Cell attachment and proliferation on high conductivity PEDOT-glycol composites produced by vapour phase polymerisation, Biomater. Sci. 1 (2013) 368–378.
[24] Y.-S. Hsiao, B.-C. Ho, H.-X. Yan, C.-W. Kuo, D.-Y. Chueh, H. Yu, et al., Integrated 3D conducting polymer-based bioelectronics for capture and release of circulating tumor cells, J. Mater. Chem. B 3 (2015) 5103–5110.
[25] L.H. Jimison, J. Rivnay, R.M. Owens, Conducting polymers to control and monitor cells, Org. Electron. Emerg. Concepts Technol. (2013) 27–67.
[26] J. Isaksson, P. Kjäll, D. Nilsson, N. Robinson, M. Berggren, A. Richter-Dahlfors, Electronic control of Ca2+ signalling in neuronal cells using an organic electronic ion pump, Nat. Mater. 6 (2007) 673–679.
[27] J. Ouyang, Solution-processed pedot:pss films with conductivities as indium tin oxide through a treatment with mild and weak organic acids, ACS Appl. Mater. Interfaces 5 (2013) 13082–13088.
[28] N. Kim, H. Kang, J.H. Lee, S. Kee, S.H. Lee, K. Lee, Highly conductive all-plastic electrodes fabricated using a novel chemically controlled transfer-printing method, Adv. Mater. 27 (2015) 2317–2323.
[29] M.N. Gueye, A. Carella, N. Massonnet, E. Yvenou, S. Brenet, J. Faure-Vincent, et al., Structure and dopant engineering in PEDOT thin films: practical tools for a dramatic conductivity enhancement, Chem. Mater. 28 (2016) 3462–3468.
[30] B. Winther-Jensen, F.C. Krebs, High-conductivity large-area semi-transparent electrodes for polymer photovoltaics by silk screen printing and vapour-phase deposition, Sol. Energy Mater. Sol. Cells 90 (2006) 123–132.
[31] J. Li, Y. Ma, In-situ synthesis of transparent conductive PEDOT coating on PET foil by liquid phase depositional polymerization of EDOT, Synth. Met. 217 (2016) 185–188.
[32] R.K. Elschner Andreas, K. Stephan, L. Wilfried, M. Udo, PEDOT principles and applications of an intrinsically, Conduct. Polym. (2011) 355.
[33] M. ElMahmoudy, S. Inal, A. Charrier, I. Uguz, G.G. Malliaras, S. Sanaur, Tailoring the electrochemical and mechanical properties of PEDOT:PSS films for bioelectronics, Macromol. Mater. Eng. 302 (2017) 1600497.
[34] X. Strakosas, B. Wei, D.C. Martin, R.M. Owens, Biofunctionalization of polydioxythiophene derivatives for biomedical applications, J. Mater. Chem. B 4 (2016) 4952–4968.
[35] T. Galán, B. Prieto-Simón, M. Alvira, R. Eritja, G. Götz, P. Bäuerle, et al., Label-free electrochemical DNA sensor using “click”-functionalized PEDOT electrodes, Biosens. Bioelectron. 74 (2015) 751–756.
[36] A. Menaker, V. Syritski, J. Reut, A. Öpik, V. Horváth, R.E. Gyurcsányi, Electrosynthesized surface-imprinted conducting polymer microrods for selective protein recognition, Adv. Mater. 21 (2009) 2271–2275.
[37] A. Biosensors, B. June, J. Daprà, N. Rozlosnik, High sensitivity point-of-care device for direct virus diagnostics high sensitivity point-of-care device for direct virus diagnostics, Biosens. Bioelectron. 49 (2013) 374–379.

[38] H. Vara, J.E. Collazos-Castro, Biofunctionalized conducting polymer/carbon microfiber electrodes for ultrasensitive neural recordings, ACS Appl. Mater. Interfaces 7 (2015) 27016–27026.
[39] B. Winther-Jensen, D.W. Breiby, K. West, Base inhibited oxidative polymerization of 3,4-ethylenedioxythiophene with iron(III)tosylate, Synth. Met. 152 (2005) 1–4.
[40] S.T. Larsen, R.F. Vreeland, M.L. Heien, R. Taboryski, Characterization of poly(3,4-ethylenedioxythiophene):tosylate conductive polymer microelectrodes for transmitter detection, Analyst 137 (2012) 1831–1836.
[41] D. Pallarola, N. Queralto, F. Battaglini, O. Azzaroni, Supramolecular assembly of glucose oxidase on concanavalin A–modified gold electrodes, Phys. Chem. Chem. Phys. 12 (2010) 8071–8083.
[42] H. Haas, H. Möhwald, Specific and unspecific binding of concanavalin A at monolayer surfaces, Thin Solid Films 180 (1989) 101–110.
[43] H. Ai, X. Huang, Z. Zhu, J. Liu, Q. Chi, Y. Li, et al., A novel glucose sensor based on monodispersed Ni/Al layered double hydroxide and chitosan, Biosens. Bioelectron. 24 (2008) 1048–1052.
[44] S. Garreau, G. Louarn, J.P. Buisson, G. Froyer, S. Lefrant, In situ Spectroelectrochemical Raman studies of poly(3,4-ethylenedioxythiophene) (PEDT), Macromolecules 32 (1999) 6807–6812.
[45] A. Schaarschmidt, A.A. Farah, A. Aby, A.S. Helmy, Influence of nonadiabatic annealing on the morphology and molecular structure of PEDOT − PSS films, J. Phys. Chem. B 113 (2009) 9352–9355.
[46] M. Reyes-Reyes, I. Cruz-Cruz, R. López-Sandoval, Enhancement of the electrical conductivity in PEDOT: PSS films by the addition of dimethyl sulfate, J. Phys. Chem. C 114 (2010) 20220–20224.
[47] F. Adar, H. Noether, Raman microprobe spectra of spin-oriented and drawn filaments of poly(ethylene terephthalate), Polymer 26 (1985) 1935–1943.
[48] S. Yang, S. Michielsen, Orientation distribution functions obtained via polarized Raman spectroscopy of poly(ethylene terephthalate) fibers, Macromolecules 36 (2003) 6484–6492.
[49] L.H. Jimison, A. Hama, X. Strakosas, V. Armel, D. Khodagholy, E. Ismailova, et al., PEDOT:TOS with PEG: a biofunctional surface with improved electronic characteristics, J. Mater. Chem. 22 (2012) 19498.
[50] J. Rivnay, S. Inal, B.A. Collins, M. Sessolo, E. Stavrinidou, X. Strakosas, et al., Structural control of mixed ionic and electronic transport in conducting polymers, Nat. Commun. 7 (2016) 1–9.
[51] K. Sanglee, S. Chuangchote, P. Chaiwiwatworakul, P. Kumnorkaew, PEDOT:PSS nanofilms fabricated by a nonconventional coating method for uses as transparent conducting electrodes in flexible Electrochromic devices, J. Nanomater. 2017 (2017) 1–8.
[52] B. Hu, D. Li, O. Ala, P. Manandhar, Q. Fan, D. Kasilingam, et al., Textile-based flexible electroluminescent devices, Adv. Funct. Mater. 21 (2011) 305–311.
[53] A.J. Bard, L.R. Faulkner, Electrochemical Methods. Fundamentals and Applications, 2nd ed., Wiley, USA, 2001.
[54] W.A. Marmisollé, M.I. Florit, D. Posadas, A formal representation of the anodic voltammetric response of polyaniline, J. Electroanal. Chem. 655 (2011) 17–22.
[55] P. Li, K. Sun, J. Ouyang, Stretchable and conductive polymer films prepared by solution blending, ACS Appl. Mater. Interfaces 7 (2015) 18415–18423.
[56] D. Cheng, F., Shang, J., and Ratner, A versatile method for functionalizing surfaces with bioactive Glycans, Bioconjug. Chem. 100 (2012) 130–134.
[57] H. Wang, F. Cheng, M. Li, W. Peng, J. Qu, Reactivity and kinetics of vinyl sulfone-functionalized self-assembled monolayers for bioactive ligand immobilization, Langmuir 31 (2015) 3413–3421.
[58] T. Hatakeyama, K. Murakami, Y. Miyamoto, N. Yamasaki, An assay for lectin activity using microtiter plate with chemically immobilized carbohydrates, Anal. Biochem. 237 (1996) 188–192.
[59] A. Lancuški, F. Bossard, S. Fort, Carbohydrate-decorated PCL fibers for specific protein adhesion, Biomacromolecules 14 (2013) 1877–1884.
[60] M. Lienemann, A. Paananen, H. Boer, J.M. De la Fuente, I. García, S. Penadés, et al., Characterization of the wheat germ agglutinin binding to self-assembled monolayers of neoglycoconjugates by AFM and SPR, Glycobiology 19 (2009) 633–643.
[61] K. Matsuoka, Biological evaluation of multivalent-type N-acetyl-D-glucosamine (GlcNAc) conjugates for wheat germ agglutinin (WGA) by the surface Plasmon resonance (SPR) method, SOJ Biochem 2 (2016) 1–7.
[62] W. Knoll, INTERFACES AND THIN FILMS AS SEEN BY BOUND ELECTROMAGNETIC WAVES, Annu. Rev. Phys. Chem. 49 (1998) 569–638.
[63] J.C. Lindon, Encyclopedia of Spectroscopy and Spectrometry, Acad. Press, San Diego, Calif, 2000.
[64] H. Tsuge, N. Osamu, O. Kazuji, Purification, properties and molecular features of glucose oxidase from Aspergillus Niger, J. Biochem. 78 (1975) 835–843.
[65] C. Bourdillon, C. Demaille, J. Moiroux, J.-M. Savéant, From homogeneous Electroenzymatic kinetics to antigen-antibody construction and characterization of spatially ordered catalytic enzyme assemblies on electrodes, Acc. Chem. Res. 29 (1996) 529–535.
[66] K.L. Prime, G.M. Whitesides, Surfaces self-assembled organic monolayers: model systems for studying adsorption of proteins at surfaces, Science 252 (2011) 1164–1167.
[67] E. Ostuni, R.G. Chapman, M.N. Liang, G. Meluleni, G. Pier, D.E. Ingber, et al., Self-assembled monolayers that resist the adsorption of proteins and the adhesion of bacterial and mammalian cells, Langmuir 17 (2001) 6336–6343.
[68] M. Hederos, P. Konradsson, B. Liedberg, Synthesis and self-assembly of galactose-terminated alkanethiols and their ability to resist proteins, Langmuir 21 (2005) 2971–2980.
[69] X. Xiao, M. Wang, H. Li, P. Si, One-step fabrication of bio-functionalized nanoporous gold/poly(3,4- ethylenedioxythiophene) hybrid electrodes for amperometric glucose sensing, Talanta 116 (2013) 1054–1059.
[70] B. Piro, L.A. Dang, M.C. Pham, S. Fabiano, C. Tran-Minh, A glucose biosensor based on modified-enzyme incorporated within electropolymerised poly(3,4-ethylenedioxythiophene) (PEDT) films, J. Electroanal. Chem. 512 (2001) 101–109.
[71] J. Park, H.K. Kim, Y. Son, Glucose biosensor constructed from capped conducting microtubules of PEDOT, Sensors Actuators B Chem. 133 (2008) 244–250.
[72] C.S. Wright, Structural comparison of the two distinct sugar binding sites in wheat germ agglutinin isolectin II, J. Mol. Biol. 178 (1984) 91–104.
[73] L.M. Shannon, E. Kay, J.Y. Lew, Peroxidase isozymes from horseradish roots. I. Isolation and physical properties, J. Biol. Chem. 241 (1966) 2166–2172.
[74] H. Zollner, Handbook of Enzyme Inhibitors, Wiley-VCH Verlag GmbH, Weinheim, Germany, 1999.
[75] S.H. Duvall, R.L. McCreery, Self-catalysis by catechols and quinones during heterogeneous electron transfer at carbon electrodes, J. Am. Chem. Soc. 122 (2000) 6759–6764.
[76] W. Li, R. Yuan, Y. Chai, L. Zhou, S. Chen, N. Li, Immobilization of horseradish peroxidase on chitosan/silica sol–gel hybrid membranes for the preparation of hydrogen peroxide biosensor, J. Biochem. Biophys. Methods 70 (2008) 830–837.
[77] Ó. Loaiza, S. Campuzano, A.G.-V. de Prada, M. Pedrero, J.M. Pingarrón, Amperometric DNA quantification based on the use of peroxidase-mercaptopropionic acid-modified gold electrodes, Sensors Actuators B Chem. 132 (2008) 250–257.
[78] S.V. Kergaravat, M.I. Pividori, S.R. Hernandez, Evaluation of seven cosubstrates in the quantification of horseradish peroxidase enzyme by square wave voltammetry, Talanta 88 (2012) 468–476.
[79] S. Laschi, I. Palchetti, G. Marrazza, M. Mascini, Enzyme-amplified electrochemical hybridization assay based on PNA, LNA and DNA probe-modified micro-magnetic beads, Bioelectrochemistry 76 (2009) 214–220.
[80] Z.M. Liu, Y. Yang, H. Wang, Y.L. Liu, G.L. Shen, R.Q. Yu, A hydrogen peroxide biosensor based on nano-Au/PAMAM dendrimer/cystamine modified gold electrode, Sensors Actuators B Chem. 106 (2005) 394–400.
[81] L. Liu, X. Jin, S. Yang, Z. Chen, X. Lin, A highly sensitive biosensor with (con a/HRP)n multilayer films based on layer-by-layer technique for the detection of reduced thiols, Biosens. Bioelectron. 22 (2007) 3210–3216.
[82] I.C. Monge-Romero, M.F. Suárez-Herrera, Electrocatalysis of the hydroquinone/benzoquinone redox couple at platinum electrodes covered by a thin film of poly (3,4-ethylenedioxythiophene), Synth. Met. 175 (2013) 36–41.
[83] S. Campuzano, M. Pedrero, P. Yáñez-Sedeño, J. Pingarrón, Antifouling (bio)materials for electrochemical (bio)sensing, Int. J. Mol. Sci. 20 (2019) 423.